

## Elevated Concentrations of U and Co-occurring Metals in Abandoned Mine Wastes in a Northeastern Arizona Native American Community

Johanna M. Blake,<sup>†</sup> Sumant Avasarala,<sup>‡</sup> Kateryna Artyushkova,<sup>§</sup> Abdul-Mehdi S. Ali,<sup>||</sup> Adrian J. Brearley,<sup>||</sup> Christopher Shuey,<sup>†</sup> Wm. Paul Robinson,<sup>†</sup> Christopher Nez,<sup>#</sup> Sadie Bill,<sup>#</sup> Johnnye Lewis,<sup>▽</sup> Chris Hirani,<sup>○</sup> Juan S. Lezama Pacheco,<sup>◆</sup> and José M. Cerrato\*,<sup>†,‡</sup>

<sup>†</sup>Department of Chemistry, MSC03 2060, University of New Mexico, Albuquerque, New Mexico 87131, United States

<sup>‡</sup>Department of Civil Engineering, MSC01 1070, University of New Mexico, Albuquerque, New Mexico 87131, United States

<sup>§</sup>Department of Chemical and Biological Engineering, MSC01 1120, University of New Mexico, Albuquerque, New Mexico 87131, United States

<sup>||</sup>Department of Earth and Planetary Sciences, MSC03 2040, University of New Mexico, Albuquerque, New Mexico 87131, United States

<sup>†</sup>Southwest Research and Information Center, P.O. Box 4524, Albuquerque, New Mexico 87196, United States

<sup>#</sup>Tachee Uranium Concerns Committee, Blue Gap, Arizona 86520, United States

<sup>▽</sup>Community Environmental Health Program, MSC09 5360, University of New Mexico, Albuquerque, New Mexico 87131, United States

<sup>○</sup>Central New Mexico Community College, Albuquerque, New Mexico 87106, United States

<sup>◆</sup>Department of Environmental Earth System Science, Stanford University, Stanford, California 94305, United States

### S Supporting Information

**ABSTRACT:** The chemical interactions of U and co-occurring metals in abandoned mine wastes in a Native American community in northeastern Arizona were investigated using spectroscopy, microscopy and aqueous chemistry. The concentrations of U ( $67\text{--}169 \mu\text{g L}^{-1}$ ) in spring water samples exceed the EPA maximum contaminant limit of  $30 \mu\text{g L}^{-1}$ . Elevated U ( $6,614 \text{ mg kg}^{-1}$ ), V ( $15,814 \text{ mg kg}^{-1}$ ), and As ( $40 \text{ mg kg}^{-1}$ ) concentrations were detected in mine waste solids. Spectroscopy (XPS and XANES) solid analyses identified U (VI), As (-I and III) and Fe (II, III). Linear correlations for the release of U vs V and As vs Fe were observed for batch experiments when reacting mine waste solids with 10 mM ascorbic acid ( $\sim\text{pH } 3.8$ ) after 264 h. The release of U, V, As, and Fe was at least 4-fold lower after reaction with 10 mM bicarbonate ( $\sim\text{pH } 8.3$ ). These results suggest that U-V mineral phases similar to carnotite [ $\text{K}_2(\text{UO}_2)_2\text{V}_2\text{O}_8$ ] and As-Fe-bearing phases control the availability of U and As in these abandoned mine wastes. Elevated concentrations of metals are of concern due to human exposure pathways and exposure of livestock currently ingesting water in the area. This study contributes to understanding the occurrence and mobility of metals in communities located close to abandoned mine waste sites.



<b>Abandoned Uranium Mine Waste (Northeastern Arizona)</b>	
<b>U in Water (Spring)</b>	<b>EPA MCL for U</b>
$67\text{--}170 \mu\text{g L}^{-1}$	$> 30 \mu\text{g L}^{-1}$

Elevated U ( $6,614 \text{ mg kg}^{-1}$ )  
Co-occurring metals:  
(e.g. As, V, Fe)

## INTRODUCTION

Uranium (U) mining operations in the United States from the 1940s to the 1980s resulted in an extensive legacy of negative environmental consequences. More than 10 000 abandoned U mine waste sites are located throughout the western United States.<sup>1</sup> On Navajo Nation, in the Four Corners region of the Southwestern United States, 1100 of these sites remain associated with more than 500 abandoned mines containing mixtures of U, arsenic (As), and other metals.<sup>1–3</sup> Concentrations of U and As in unregulated water sources used for

drinking by livestock and residents who lack access to regulated water sources on Navajo Nation have been found to exceed the U.S. Environmental Protection Agency Maximum Contaminant Limit (USEPA MCL).<sup>2</sup> Although the high concentrations of metals in water sources could be attributed to naturally

Received: March 19, 2015

Revised: June 20, 2015

Accepted: June 24, 2015

Published: July 9, 2015



occurring geological characteristics or leaching from abandoned uranium mine wastes in these communities, limited scientific studies have addressed the sources of metals and their potential mobility in abandoned mine wastes in Navajo Nation. For example, the USEPA has assessed the U and As concentrations in Tuba City and Monument Valley, AZ; Mexican Hat, UT and Shiprock and Church Rock, NM, all on Navajo Nation.<sup>4</sup> Another study from Kamp and Morrison<sup>5</sup> used chemical and isotopic signatures to distinguish the source of uranium in groundwater near Shiprock, NM. The United States Geological Survey (USGS) has also published reports on water quality in Monument Valley, AZ,<sup>6</sup> and deLemos et al.<sup>7</sup> reported the rapid dissolution of a soluble uranyl phase near Church Rock, NM.

Toxicity of both U and As is well documented in human exposure by inhalation and ingestion.<sup>8,9</sup> Uranium has long been recognized as a kidney toxicant<sup>9</sup> but also has been linked to adverse developmental outcomes in animals.<sup>10</sup> Arsenic is a known carcinogen but also affects fetal development, the central nervous system, and the circulatory system.<sup>8</sup> Additionally, recent studies in Navajo communities have linked exposures to mine wastes with an increased likelihood of developing one or more chronic diseases including hypertension, kidney disease, and diabetes.<sup>11</sup> The toxicity of V due to ingestion or inhalation pathways has not been widely studied.<sup>12–15</sup> However, a synergistic cardiovascular effect was observed in animal studies assessing the toxicity of V and Ni due to inhalation of ambient particulate matter.<sup>13</sup> Additionally, V can interfere with enzymatic systems such as ATPases and ribonucleases and lungs can absorb soluble vanadium compounds and are the main organ affected by vanadium toxicity.<sup>12,16</sup>

Mine waste sites located in Native American communities have been overlooked because of low population densities and the remoteness of the waste sites themselves. A clear example is the Blue Gap/Tachee Chapter of the central Navajo Nation in northeastern Arizona where more than a dozen mining sites were operated starting in the 1950s, and were abandoned when mining operations ceased in the late 1960s. Mine wastes were produced from conventional underground and open-pit mining and were not subject to regulatory controls. However, uranium mill tailings (the wastes left over from the processing of ore for its U content) have been regulated by the federal government and states under authority of the Atomic Energy Act since 1978.<sup>17</sup> Reclamation of mine wastes and environmental restoration of abandoned mine sites are now being addressed by the USEPA, in collaboration with states and tribes, under authority of the federal Superfund law<sup>3</sup> or under state laws regulating hardrock mining. Thousands of abandoned uranium mine sites that exist in the western United States have not yet been systematically characterized.<sup>1</sup>

A variety of biogeochemical and physical processes could control the mobility and fate of U, As, and other co-occurring metals in abandoned mine wastes. Some key parameters that control mechanisms of adsorption, dissolution, precipitation of secondary minerals, and aqueous complexes include pH, Eh, temperature, and elemental composition of the system.<sup>18–20</sup> The occurrence of U(IV) is common in reduced subsurface environments; examples of U(IV) phases are more labile monomeric U(IV)<sup>21–24</sup> and uraninite, whose solubility can be orders of magnitude lower than other uranium mineral phases.<sup>25–27</sup> Under surface oxic conditions and environmentally relevant pH values, U(VI) is the most soluble and mobile form.<sup>28,29</sup> For instance, U(VI) can form pH-dependent

aqueous complexes with carbonate as uranyl-carbonates, accounting for 60–80% of the soluble U(VI) species at a circumneutral pH.<sup>28,30,31</sup> In addition, U(VI) can adsorb to Fe and Mn oxides<sup>32–35</sup> or occur in mineral phases such as phosphates, vanadates, and silicates.<sup>36–38</sup> Uranyl vanadates, such as carnotite [ $K_2(UO_2)_2V_2O_8$ ] and tyuyamunite [ $Ca(UO_2)_2(VO_4)_2 \cdot nH_2O$ ], are commonly occurring mineral phases under oxidizing environments typical of abandoned mine wastes with abundant concentrations of U and V.<sup>38–40</sup> Arsenic may exist in different oxidation states (e.g., –I, 0, I, III, and V), among which As(III) and As(V) are most commonly observed in the environment.<sup>41–44</sup> The reduced form As(III) is generally the most mobile in the environment, especially below pH 7–8.<sup>45–47</sup> Both As(III) and As(V) can adsorb to iron oxides (ferrihydrite, goethite, or hematite) or iron-bearing clay minerals (illite, saponite, or kaolinite with oxidized iron) at environmentally relevant pH values and conditions.<sup>45,46,48,49</sup> Additionally, As(III) and As(V) can occur in primary mineral phases, such as arsenopyrite ( $FeAsS$ ), orpiment ( $As_2S_3$ ), and realgar ( $As_4S_4$ ), and secondary mineral phases, such as scorodite ( $FeAsO_4 \cdot 2H_2O$ ) or conichalcite ( $CaCu(AsO_4)_2(OH)$ ).<sup>50–52</sup> In many instances, U and As can be found in an environmental system as mixtures of two or more of these mineral phases. Examples of these are U(VI) adsorbed to ferrihydrite, As(V) or As(III) adsorbed to goethite, and the mineral trogerite ( $UO_2 \cdot HAsO_4 \cdot 4H_2O$ ).<sup>50</sup> Limited studies have focused on understanding the chemical interaction and mechanisms controlling the potential release of metal mixtures of U, As, and co-occurring elements from mine wastes into water sources.<sup>50,53</sup>

The main objective of this study was to assess the presence and chemical interaction of U and other co-occurring metals in soils in the Claim 28 abandoned mine waste site and in adjacent and nearby springs in Blue Gap/Tachee Chapter of the Navajo Nation in northeastern Arizona. The study was initiated in response to repeated concerns of community members about the potential health impacts of living close to this and other abandoned mines. We conducted spectroscopy, microscopy, diffraction, and aqueous chemistry analyses to assess the chemical composition and structure of abandoned mine waste solids. Through batch laboratory experiments, we assessed interfacial processes affecting metal release under environmentally relevant conditions. The results from this investigation contribute to a better understanding of the metal contents of the wastes and the chemical interactions that affect metal occurrence and mobility.

## MATERIALS AND METHODS

**Materials.** Samples of abandoned mine waste solids, soil, and water from adjacent and nearby springs were collected from the Claim 28 abandoned uranium mine in 2014. The mine waste site is located within 1 km of homes of Blue Gap/Tachee community members (Supporting Information, Figure S1). A total of seven samples (four water and three solid samples) were collected in two sampling trips in January and June 2014. Among the collected water samples, WS1 and WS2 were collected from a seep flowing out of the mine waste site at Claim 28. This seep was identified by local residents whose families had used the location for drinking water and livestock water in the 1960s and 1970s. Two other water samples, WS3 and WS4, were collected from a spring (locally called Waterfall Spring) located 5 km northeast of the abandoned mine site at the head of a dendritic drainage pattern. Unlike the seep, this

spring flows out of bedrock. Water samples were collected in precleaned, 250 mL polypropylene bottles for transport to the laboratory. A calibrated portable pH meter (Yellow Springs Instrument Co., Model 63) was used to measure the pH and temperature of the waters immediately after collection.

Throughout the study, the three solid samples are referred to as mine waste 1 (MW1), mine waste 2 (MW2), and baseline reference soil (BRS). Sample MW1 is a solid sample from an erosion channel within the Claim 28 mine waste. Sample MW2 is a solid sample collected from a similar location in the surface of the Claim 28 site from where sample MW1 was collected. Note that both samples MW1 and MW2 are comparable given that, even though they were collected on different dates, they were obtained from the Claim 28 mine waste site. Sample BRS consists of soil located 2 km from the abandoned mine waste site on local range land that had not been impacted by mining activities. The mine waste solids and soil samples were collected from the top 30 cm of each location under surface oxic conditions and placed into labeled gallon plastic bags. Gamma ( $\gamma$ ) radiation measurements, using a calibrated Ludlum Model 19 MicroR Meter and a Safecast bGeigie Geiger counter helped classify the three solid samples as mine wastes and baseline reference soil (Supporting Information, Table S1). The BRS sample was designated as a baseline reference soil based on a maximum surface  $\gamma$  radiation rate (13  $\mu\text{R}/\text{h}$ ) typical of rates observed in areas of the Navajo Nation not impacted by mining or other human activities that may technologically mobilize naturally occurring radioactive materials.

**Acid Extractable Procedure.** To assess the acid extractable elements from the mine waste samples, an acid digestion was performed. The digestion involved addition of 3 mL of concentrated hydrofluoric acid (HF), 3 mL concentrated nitric acid ( $\text{HNO}_3^-$ ) and 5 mL concentrated hydrochloric acid (HCl) into 50 mL Teflon digestion tubes with  $2.000 \pm 0.002$  g of  $<63\ \mu\text{m}$  soil sample. All reagents used were high purity. The digestion tubes were then heated in a Digi prep MS SCP Science block digester at  $95\ ^\circ\text{C}$  for 2 h. Following heating, acid extracts were diluted to 50 mL and filtered through a  $0.45\ \mu\text{m}$  filter to remove suspended solids from samples before analysis.

**Inductively Coupled Plasma (ICP).** Water samples and extracts from the acid digestion of the solid samples were measured for elemental concentrations using a PerkinElmer Optima 5300DV Inductively Coupled Plasma-Optical Emission Spectrometer (ICP-OES), with a detection limit of  $<0.5\ \text{mg L}^{-1}$ . Trace elemental concentrations were measured with a PerkinElmer NexION 300D (Dynamic Reaction Cell) Inductively Coupled Plasma-Mass Spectrometer (ICP-MS), with a detection limit of  $<0.5\ \mu\text{g L}^{-1}$ . Both ICPs are calibrated with a five-point calibration curve, and QA/QC measures are taken to ensure quality results.

**Procedure for Batch Experiments.** Batch experiments were performed to understand the mechanisms that control the release of labile metals from solid mine waste samples. The experiments were performed using 10 mM bicarbonate and ascorbic acid solutions at a pH of 8.3 and 3.8, respectively, to assess the mechanisms based on release times using environmentally relevant reactants. These pH values and concentrations were carefully chosen to closely mimic the buffering capacity and pH of the aqueous samples collected from the abandoned mine waste site. The dry solid sample was sieved using U.S. standard sieve series number 230 ( $63\ \mu\text{m}$ ), and  $0.1000 \pm 0.0005$  g of replicate samples were weighed into 50 mL centrifuge tubes. We used 18 M'Ω deionized water to

prepare 10 mM bicarbonate and ascorbic acid solutions. Then, 50 mL of reagent was volumetrically added to the samples and exposed to a continuous gentle shaking for 264 h. The experiment was performed for 264 h collecting 2 mL samples at time periods of 0.5, 1, 2, 6, 24, 48, 96, and 264 h. This process was repeated for MW1, MW2, and BRS in triplicate. The extracts were filtered using a  $0.45\ \mu\text{m}$  syringe filter and accordingly diluted for analysis by ICP-OES and an ICP-MS.

**Solid Characterization.** Mine waste samples and sediments were analyzed using X-ray diffraction (XRD), scanning electron microscopy (SEM), X-ray fluorescence (XRF), X-ray photoelectron spectroscopy (XPS), and X-ray absorption spectroscopy (XAS). Additional technical details of these methods are described in the Supporting Information.

## RESULTS AND DISCUSSION

**Elemental Content of Water Samples.** Elevated concentrations of U, ranging between  $67$  and  $169\ \mu\text{g L}^{-1}$ , were measured in water sources on the abandoned mine waste and 5 km away from the Claim 28 mine waste location that was sampled for this study. These concentrations are 2–5 times higher than the USEPA of  $30\ \mu\text{g L}^{-1}$  for regulated drinking water.<sup>3</sup> The pH of the samples collected from a seep on the mine waste site (WS1 and WS2) was 3.8 in both samples, with alkalinity below the method detection limit, while the pH of samples collected 5 km northeast of the mine waste from a developed spring flowing out of bedrock (WS3 and WS4) was 7.2 and 7.4, with alkalinities ranging from  $135$  to  $430\ \text{mg L}^{-1}$  as  $\text{CaCO}_3$  (Table 1). Our results are consistent with a previous

**Table 1. Aqueous Elemental Content and pH of Water Samples<sup>a</sup>**

parameters	Seep 1 (WS1)	Seep 2 (WS2)	Spring 1 (WS3)	Spring 2 (WS4)
Al	56 300	60 500	BDL <sup>b</sup>	BDL
As	5.7	5.7	6.6	9.6
U	163	169	67	135
K	16 400	16 400	4500	6300
V	115	171	156	158
Fe	22	22	BDL	BDL
pH	3.8	3.8	7.2	7.4
alkalinity	<0.01	<0.01	430	135

<sup>a</sup>Aqueous elemental content measured with ICP-OES and ICP-MS). All concentrations in  $\mu\text{g L}^{-1}$ , except for pH (units) and alkalinity ( $\text{mg L}^{-1}$  as  $\text{CaCO}_3$ ). <sup>b</sup>BDL = below detection limit.

study performed by the USEPA that considered the same location from which sample WS3 for this study was obtained, reporting a concentration of  $92.6\ \mu\text{g L}^{-1}$  U.<sup>4</sup> Arsenic concentrations in all four water samples ranged from  $5.7$  to  $9.6\ \mu\text{g L}^{-1}$ . These concentrations are close to the As MCL of  $10\ \mu\text{g L}^{-1}$ .<sup>54</sup> Aqueous concentrations of vanadium are consistent across all four water samples: V ranged from  $115\ \mu\text{g L}^{-1}$  to  $171\ \mu\text{g L}^{-1}$  in the mine-seep samples and from  $156$  to  $158\ \mu\text{g L}^{-1}$  in the developed spring samples. The concentrations of V observed in this study are comparable to those reported for the U.S. Department of Energy (DOE) site in Rifle, CO (mean V concentration  $145.9\ \mu\text{g L}^{-1}$ ).<sup>55</sup> Iron concentrations also reported by ICP-OES are as low as  $22\ \mu\text{g L}^{-1}$  for samples WS1 and WS2 but were below detection limit (BDL) for samples WS3 and WS4.

Table 2. Elemental Content of Solid Samples Determined by X-ray Fluorescence (XRF) and ICP-OES

samples	elemental content ( $\mu\text{g g}^{-1}$ )						
	Al	As	U	K	V	Fe	S
baseline reference soil (BRS)	52 129	BDL <sup>a</sup>	BDL	36 678	BDL	26 739	1339
mine waste 1 (MW1)	69 533	20 <sup>b</sup>	2248	54 072	15 814	15 259	223
mine waste 2 (MW2)	59 730	40 <sup>b</sup>	6614	69 604	4328	3511	1834

<sup>a</sup>BDL = below detection limit. The detection limit for U and As is  $60 \mu\text{g g}^{-1}$  and for V is  $200 \mu\text{g g}^{-1}$ . <sup>b</sup>ICP-OES results.

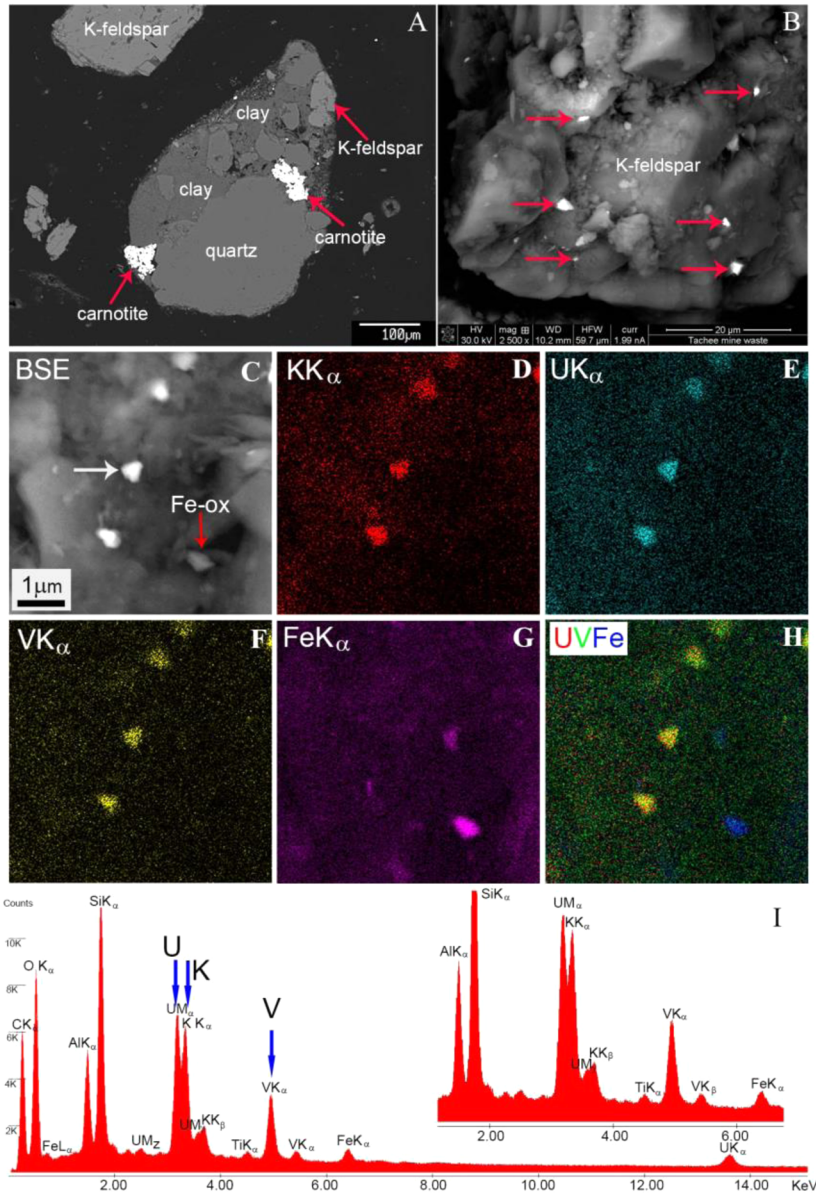


**Figure 1.** SEM and EDS characterization of sample MW1. (A) BSE image of polished sample showing rock fragment with aggregates of a U–V phase (red arrows) associated with quartz, K-feldspar, and clay. (B) BSE image of dispersed sample of MW1 showing micron-sized grains of a U–V phase on the surfaces of quartz and feldspar grains. (C) BSE image of a U–V phase (white arrow) on the surface of K-feldspar. Fe oxide or oxyhydroxide (Fe-ox) grain is arrowed (red). (D, E, F, and G) Elemental X-ray maps for K, U, V, and Fe of region shown in C, showing that K, U, and V occur in the high Z contrast grains. (H) Composite X-ray map of (red) U, (green) V, and (blue) Fe, showing (yellow) correlation of U and V in the submicron grains, and (blue, lower right) iron is uncorrelated and occurs in distinct grains. (I) EDS spectrum from a of a U–V phase on K-feldspar showing distinct K, U, and V peaks; (inset) enlarged region of spectrum. The Si and Al peaks are from the K-feldspar substrate which also contributes to the K peak.

**Bulk Elemental Content of Abandoned Mine Waste Solid Samples.** Elevated U concentrations, ranging from 2200 to  $6600 \text{ mg kg}^{-1}$ , were measured in abandoned mine waste solid samples through XRF bulk analysis. While the mine waste

U concentrations are 2–3 orders of magnitude greater than the crustal average<sup>1</sup> of  $2.78 \text{ mg kg}^{-1}$ , the BRS concentration is BDL of  $60 \text{ mg kg}^{-1}$  U on the XRF. Arsenic is BDL on the XRF for all samples. ICP-OES measurements for arsenic concentrations are

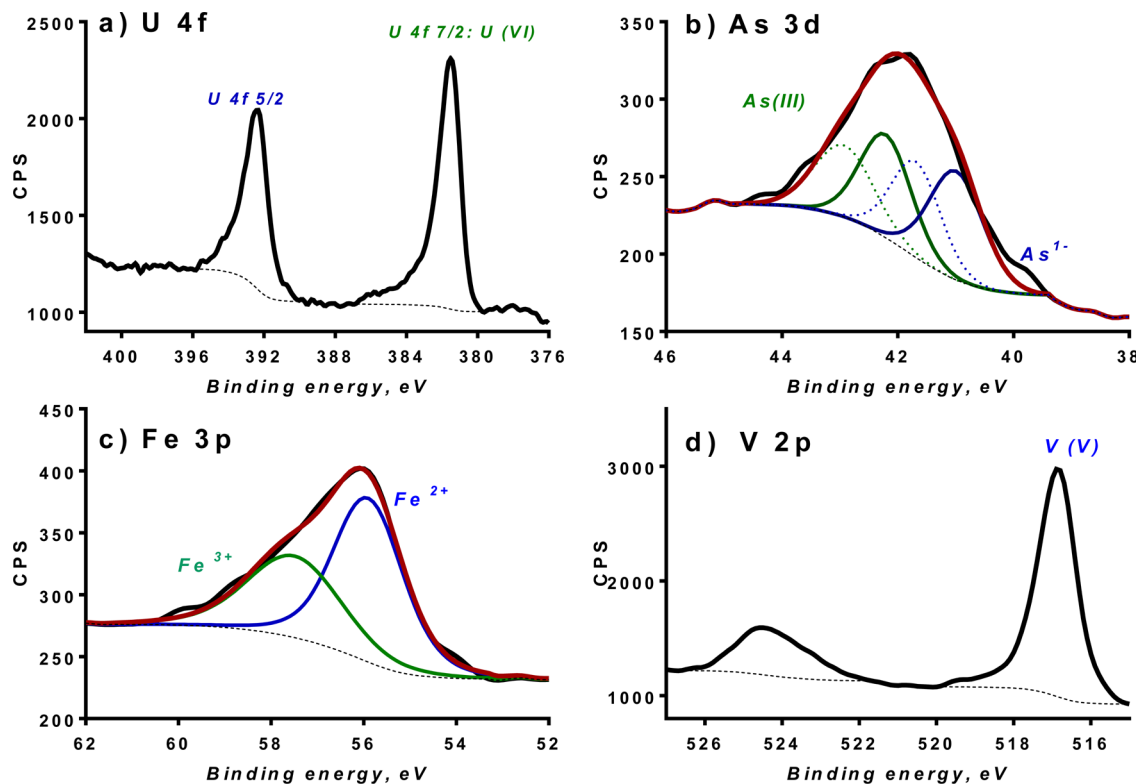


**Figure 2.** High-resolution XPS spectra representative of the sample (MW1). Uranium and vanadium are present as VI and V chemical states in all the analyzed areas. In some areas, As is present as As(III), and in others, it is present as a reduced form (As(-I)). Both  $\text{Fe}^{2+}$  and  $\text{Fe}^{3+}$  are present in samples. The black line represents experimental spectra obtained. The red line represents the fitted curve resulting from sum of individual peaks used in fitting. The results of quantitative analysis of the spectra are reported in Table S3 (Supporting Information) for samples from two different mine waste areas.

20–40 mg kg<sup>-1</sup> (crustal average 1.7 mg kg<sup>-1</sup>)<sup>52</sup> for mine wastes and BDL for the reference soil. Additional XRF results are shown in Table 2. The BRS Al and S concentrations are similar to the mine waste concentrations, K concentrations are 2 times lower in the BRS deposit, and Fe is up to 2 times higher in the BRS. The elemental concentrations in the BRS further confirm that this sample is representative of background conditions not impacted by mining activities.

**Mineralogy of Mine Waste Samples.** X-ray diffraction patterns from the mine waste solid samples show that the major mineralogical constituents are quartz ( $\text{SiO}_2$ ; 59%) potassium feldspar ( $\text{KAlSi}_3\text{O}_8$ ; 34%), and kaolinite ( $\text{Al}_2\text{Si}_2\text{O}_5(\text{OH})_4$ ; 7%; Supporting Information, Figure S2). These data are supported by SEM backscattered electron (BSE) imaging and SEM/EDX (Figure 1A). In addition to these major phases, BSE imaging and EDS X-ray mapping also show the presence of a U- and V-rich phases that occur as aggregates (up to 80  $\mu\text{m}$  in size) and individual grains as small as 200 nm (Figure 1B,C). X-ray mapping (Figure 1D–H) and qualitative EDS (Figure 1I) analysis show that the main U–V-rich phase also contains elevated concentrations of K, suggesting that it is most likely to be the uranyl vanadate, carnotite ( $\text{K}_2(\text{UO}_2)_2(\text{VO}_4)_2 \cdot 1\text{--}3\text{H}_2\text{O}$ ) (Figure 1B). Some analyses also show the presence of variable concentrations of Ca that may be due to the presence of the Ca-bearing uranyl vanadates, tyuyamunite ( $\text{Ca}(\text{UO}_2)_2(\text{VO}_4)_2 \cdot 5\text{--}8\text{H}_2\text{O}$ ), metatyuyamunite ( $\text{Ca}(\text{UO}_2)_2(\text{VO}_4)_2 \cdot 3\text{--}5\text{H}_2\text{O}$ ), or both.

These data from the mine waste solids are consistent with the known mineralogy of the ore-bearing formation. The U ore in this area is hosted in tabular and lenticular bodies within the

Cretaceous Mesa Verde Group, specifically the Rough Rock Sandstone (formerly named the upper sandstone unit of the Toreva Formation<sup>56</sup>), an arkosic sandstone composed of quartz, potassium feldspar, and clays.<sup>57</sup> The mineralogy of U-bearing ore in this area is dominated by U- and V-rich minerals, including carnotite, tyuyamunite, melanovanadite, and vanadium-rich clays.<sup>57</sup>

**XPS Surface Analyses for Oxidation States.** The presence of 100% U(VI) and 100% V(V) (based on the positions of the  $\text{U } 4f_{7/2}$  and  $\text{V } 2p_{3/2}$  peaks) in the near-surface region of samples MW1 and MW2 was determined by high resolution U 4f and V 2p XPS spectra (Figure 2; and Supporting Information, Table S2). Curve fitting analyses of the As 3d region indicate that sample MW1 contains 83% As(III) and 17% of As(-I) (Figure 2; Supporting Information, Table S3). The presence of 72% Fe(II) and 28% Fe(III) was also identified in sample MW1 (Figure 2; Supporting Information, Table S3 and Figure S4), with Fe(II) as the dominant oxidation state in MW1 (Figure 2). In sample MW2, 100% As (III) was detected with 50% Fe(II) and 50% Fe(III). In contrast, the BRS sample contains 72% Fe(III) and 28% Fe(II) (Supporting Information, Table S3), with concentrations of As and U below detection limit (Supporting Information, Table S3). These results suggest that a higher percentage of Fe(II) is present when there is reduced As in mine waste samples. The speciation of As in gold mine wastes has been quantified with different characterization techniques and found to be a combination of approximately 20% reduced As (likely as arsenopyrite and arsenical pyrite) and 80% as oxidized As.<sup>44</sup> Other researchers reacted arsenopyrite with

waters from a waste rock pile, reported a combination of Fe(III) from oxidized surface layers and Fe(II) from arsenopyrite, which contributed to the total Fe 2p XPS spectra.<sup>43</sup> In our study, variable atomic percentages of U 4f, V 2p, As 3d, and Fe 3p was determined by XPS survey scans for samples MW1 and MW2 (Supporting Information, Table S2), indicating notable physical and chemical heterogeneity between mine waste samples MW1 and MW2, collected at different locations on the Claim 28 site.

**X-ray Absorption Fine Structure (XAFS) Bulk Analyses to Determine Oxidation State and Molecular Coordination.** The predominance of U(VI) in MW1 is confirmed by direct comparison to the XANES spectra of U(IV) in  $\text{UO}_{2.00}$  and U(VI) in carnotite (Figure 3A). The typical shape of the

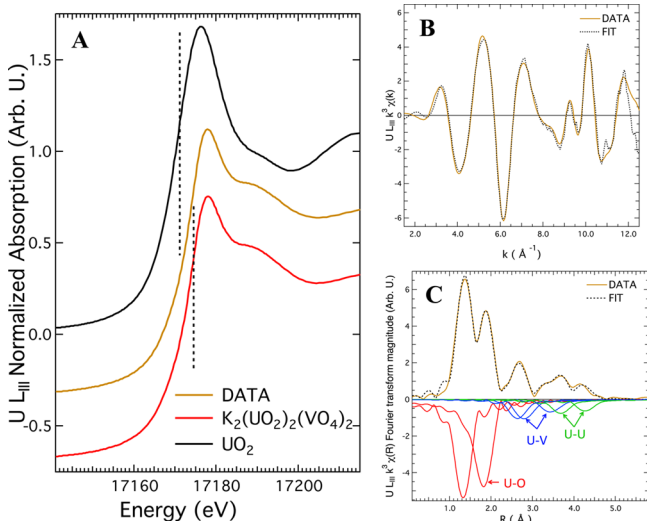


**Figure 3.** (A, dark mustard curve) Normalized XANES spectra for MW1, (black curve) reference spectra for U(IV),  $\text{UO}_{2.00}$  stoichiometric uraninite, (red curve) and U(VI), carnotite  $[\text{K}_2(\text{UO}_2)_2\text{V}_2\text{O}_8]$ , are shown for comparison. (B) MW1 background subtracted EXAFS (dark mustard curve); (C) Fourier transform magnitude and shell by shell fit (dashed). Individual scattering paths included in the fit (red, U–O; blue, U–V; and green, U–U pairs) are displayed in panel C in an inverted scale. The dotted lines are located at the inflection points of U(IV) and U(VI) standard compounds and were included in the figure as aids for the eye to distinguish the energy shift between the different Uranium species.

white line on the XANES spectra and the associated edge shift, including the higher energy multiple scattering shoulder consistent with U(VI), is remarkably similar to that of carnotite. Coordination numbers found through EXAFS fits (Figure 3B,C; Supporting Information, Table S5) confirm the presence of a uranyl vanadate local structure motif, with coordination similar to that found in carnotite or tyuyamunite. No additional pair correlations that would indicate the presence of uranyl phosphate or other carbonate mineral phases were found to be present in the EXAFS spectra.

**Batch Experiments under Environmentally Relevant Conditions.** The release of U into solution was observed from batch experiments using 10 mM  $\text{HCO}_3^-$  (pH 8.3) and 10 mM ascorbic acid (pH 3.8; Figure 4). The experimental conditions used represent environmentally relevant pH and alkalinity values found in springs sampled from the mine waste region. The pH value of 8.3 is characteristic of the spring flow out of bedrock while the pH 3.8 represents a seep from mine waste.

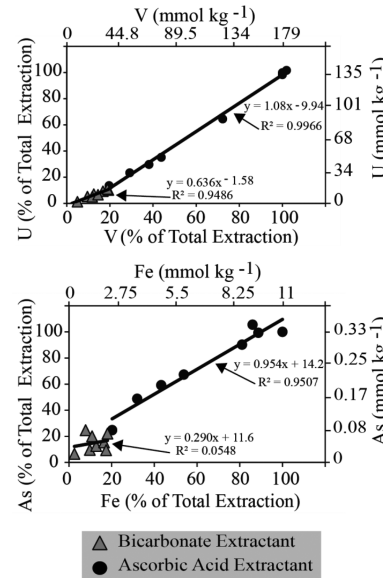


**Figure 4.** U, V, As, and Fe trends for dissolution experiments in (●) ascorbic acid (pH 3.8) and (gray △) bicarbonate solution (pH 8.3); (top) correlation between percentage release of U and V, and (bottom) correlation between percentage release of As and Fe. Aliquots were sampled from 0.5 to 264 h for both the ascorbic acid and bicarbonate solutions.

Within 1 h of reaction with the bicarbonate solution, 1700 mg  $\text{kg}^{-1}$  of U was released, which is 40% of the total U released from the solid. The concentration of U released after 264 h with the bicarbonate solution was similar to the concentration released after 0.5 h with the ascorbic acid solution. Desorption and complexation contribute to readily release mobile species of U and V from mine waste solids exposed to 10 mM  $\text{HCO}_3^-$  at pH 8.3. A similar release pattern is observed in the first 0.5 h of reaction with ascorbic acid. The release of U(VI) into water has been related to natural oxidizing and carbonate-rich conditions,<sup>27,28,40</sup> similar to experiments performed in the laboratory and in the field. Additionally, a linear relationship between U and V exists ( $R^2 = 0.9486$ ) for the bicarbonate solution results (Figure 4), which indicates that the two elements are cohosted in the same mineral.

A linear relationship also exists between U and V ( $R^2 = 0.9966$ ) for the ascorbic acid results (Figure 4), which show a proportionate release of U and V likely the result of congruent dissolution of carnotite. The dissolution of carnotite is controlled mainly by the low pH of 3.8 rather than complexation with ascorbate, given that the  $pK_{\text{a}1}$  of ascorbic acid is 4.10. At pH 3.8, we expect that the solution will consist of 67% ascorbic acid and only 33% ascorbate, so complexation of metals with ascorbate will not play a predominant role. Higher dissolution of carnotite was observed at pH 4 compared with pH 8 in another study.<sup>38</sup>

The release rate of As using 10 mM bicarbonate was 4–5 times lower than with the 10 mM ascorbic acid. Similar to the behavior of U release, the concentration of As released after 0.5 h of reaction with ascorbic acid is only reached after 264 h of reaction with bicarbonate. After 2 h of reaction with bicarbonate, the As concentration released from MW1 was 1.5 times greater than the crustal average of 1.7 mg  $\text{kg}^{-1}$ .<sup>52</sup> The relationship between As and Fe release with the bicarbonate solution is not linear ( $R^2 = 0.0548$ ), indicating that under these conditions the release of these metals is not caused by an As–

Fe bearing mineral phase. Nonlinear release could also occur due to significant dissolution and reprecipitation, or dissolution and readsorption. However, the relationship is linear with the ascorbic acid experiment ( $R^2 = 0.9507$ ) (Figure 4). As noted earlier, it is expected that at pH 3.8 the solution will contain 67% ascorbic acid and only 33% ascorbate, so complexation of metals or reduction by ascorbate will not play a predominant role. Thus, it is likely that the release of As and Fe at pH 3.8 is controlled by an As–Fe bearing phase. This result is consistent with XPS analyses which suggest the possibility of an As and Fe mineral association. Arsenic-Fe-bearing phases can play an important role in the mobility of As in these abandoned mine wastes.<sup>41,43</sup> The early release of some Fe and As with bicarbonate and the nonlinear nature of the relationship indicates that these two elements are weakly bound leading to three possibilities: (1) easily mobile As from Fe oxides or Fe oxyhydroxides; (2) weakly bound, easily oxidizable As–Fe phases due to their proportionate release; or (3) a combination of 1 and 2. These results are consistent with the findings reported in other studies.<sup>42,51</sup> For instance, when arsenopyrite reacted with waters from a waste rock pile, reduced arsenic was still present in the surface of oxidized arsenopyrite due to diffusion of reduced As from the unoxidized interior of the mineral.<sup>41,43,44</sup> While our XPS analyses suggest that reduced As(–I) is present in mine waste sample MW1, additional research is needed to identify arsenopyrite or As-bearing Fe-oxide mineral phases.

**Environmental Implications.** The elevated concentrations of U and co-occurring metals at the Claim 28 abandoned uranium mine waste site represent a concern for communities living nearby. Metals contained in these abandoned mine wastes could potentially be released through runoff and human exposure pathways which include consumption of livestock currently ingesting water in the area. The results in this study present for the first time a characterization of the concentrations of U and co-occurring metals, and the chemical interactions in and around the Claim 28 site that could affect the potential release of these constituents. The information gathered will help community members and stakeholders influence public policy to make informed decisions about the adequate management of abandoned mine waste sites in the Blue Gap/Tachee community. The wastes at the Claim 28 site have concentrations of U ranging from 0.22 to 0.66 wt %, that are typical of ore grades mined throughout the Colorado Plateau since the late 1940s.<sup>58,59</sup> Furthermore, U concentrations in the mine wastes analyzed in this study are 4–11 times greater than the concentration that defines “source material” under NRC regulations,<sup>60</sup> referring to ores containing 0.05 wt % U, or 500 mg kg<sup>-1</sup>. Findings from this study suggest that uranyl vanadates such as carnotite and As–Fe-bearing phases control the availability of U and As in these abandoned mine wastes. Batch experiments reveal the mobility of U and As from the mine waste sediments exposed to the pH values and complexing agents used in this study. It is also worth noting that our XPS analyses suggest that As(III) was predominant in samples MW1 and MW2; As(III) is a toxic and potentially mobile form of As. Carnotite occurs as grains that can be as small as 200 nm, and so, they have a large surface-to-volume ratio, which will enhance dissolution rates. This is very important for the rapid release of these elements when water is available. These results provide new insights to the limited literature related to chemical interactions of U, As, and other metal mixtures in environmentally relevant systems. Our study

suggests that the dissolution and reactivity of U–V phases (e.g., carnotite) in abandoned mine wastes are important mechanisms controlling the mobility of U in water sources close to abandoned mine waste sites with similar geological characteristics to that of the Claim 28 site. It is also possible that adsorbed phases and other secondary precipitate phases that have not yet been identified in this study control the mobility of U and As under field conditions.

The water sources sampled in this study, which contained U concentrations 2–5 times higher than the USEPA MCL, were previously used by the community for human consumption. No data are available to assess the concentrations of these metals in the water source at the Claim 28 mine waste site during the active mining period when community members were unaware of the risks by ingestion of these water sources. The water source located 5 km to the northeast of the Claim 28 mine waste site is still used for animal consumption. These metals could be mobilized in water under environmentally relevant conditions tested in our laboratory for experiments conducted at pH 3.8 and 8.3. Both the inhalation and ingestion pathways could result in significant exposures with mobilization of even relatively low percentages of the waste material given the high concentrations of metals and small grain sizes available documented in our investigation. Understanding exposure pathways related to ingestion of particulate material from abandoned uranium mine wastes is an important subject for future research. This study demonstrates that mine wastes are significant potential sources of heavy metals that can be released rapidly in the water system and, hence, can present a major source of potential exposure to metals to people living close to abandoned mine waste sites.

## ASSOCIATED CONTENT

### S Supporting Information

Additional tables, figures, and description of solid sample analyses. The Supporting Information is available free of charge on the ACS Publications website at DOI: 10.1021/acs.est.Sb01408.

## AUTHOR INFORMATION

### Corresponding Author

\*E-mail: jcerrato@unm.edu. Telephone: (001) (505) 277-0870. Fax: (001) (505) 277-1918.

### Notes

The authors declare no competing financial interest.

## ACKNOWLEDGMENTS

The authors would like to acknowledge the existing partnership with the Blue Gap/Tachee Chapter and Navajo Nation Environmental Protection Agency (NNEPA). Special thanks to Michael Spilde (SEM analyses), Virgil Luth (XRD analyses), Ernesto Echeverria, and Fernando Echeverria for assistance with batch experiments. Thanks to Dr. Michael F. Hochella, Jr., and three anonymous reviewers for their thoughtful comments which contributed to significantly improve this manuscript. Part of this research was carried out at the Stanford Synchrotron Radiation Lightsource, a national user facility operated by Stanford University on behalf of the US DOE-OBER. Funding for this research was provided by the National Science Foundation under New Mexico EPSCoR (Grant Number #IAA-1301346) and CREST (Grant Number 1345169). Any opinions, findings, and conclusions or recommendations

expressed in this publication are those of the author(s) and do not necessarily reflect the views of the National Science Foundation.

## ■ REFERENCES

- (1) USEPA *Technical Report on Technologically Enhanced Naturally Occurring Radioactive Materials from Uranium Mining Vol. 1: Mining and Reclamation Background*; U.S. Environmental Protection Agency, Office of Radiation and Indoor Air, EPA 402-R-08-005: Washington, D.C., April, 2008a.
- (2) USEPA *Addressing uranium contamination on the Navajo Nation*. U.S. Environmental Protection Agency, Pacific Southwest, Region 9: San Francisco, CA, 2015.
- (3) USEPA, *Federal actions to address impacts of uranium contamination in the Navajo Nation: Five-year plan summary report*. U.S. Environmental Protection Agency, Pacific Southwest, Region 9: San Francisco, CA, 2013.
- (4) USEPA, Abandoned uranium mines and the Navajo Nation: Navajo Nation AUM screening assessment report and atlas with geospatial data. U.S. Environmental Protection Agency, Region 9 Superfund Records Center: Los Angeles, CA, 2007.
- (5) Kamp, S. D.; Morrison, S. J. Use of chemical and isotopic signatures to distinguish between uranium mill-related and naturally occurring groundwater constituents. *Groundwater* **2014**, *34* (1), 68–78.
- (6) Longsworth, S. A. *Geohydrology and water chemistry of abandoned uranium mines and radiochemistry of spoil-material leachate, Monument Valley and Cameron areas, Arizona and Utah*. U.S. Geological Survey: Reston, VA, 1994.
- (7) deLemos, J. L.; Bostick, B. C.; Quicksall, A. N.; Landis, J. D.; George, C. C.; Slagowski, N. L.; Rock, T.; Brugge, D.; Lewis, J.; Durant, J. L. Rapid dissolution of soluble uranyl phases in arid, mine-impacted catchments near Church Rock, NM. *Environ. Sci. Technol.* **2008**, *42* (11), 3951–3957.
- (8) U.S. Department of Health, *Toxicological Profile for Arsenic*. Agency for Toxic Substances and Disease Registry (U.S.): Atlanta, GA, 2000.
- (9) Keith, S.; Faroone, O.; Roney, N.; Scinicariello, F.; Wilbur, S.; Ingberman, L.; Llados, F.; Plewak, D.; Wohlers, D.; Diamond, G. *Toxicological Profile for Uranium*. Agency for Toxic Substances and Disease Registry (U.S.): Atlanta, GA, 2013.
- (10) Domingo, J. L. Reproductive and developmental toxicity of natural and depleted uranium: a review. *Reprod. Toxicol.* **2001**, *15* (6), 603–609.
- (11) Hund, L.; Bedrick, E. J.; Miller, C.; Huerta, G.; Nez, T.; Ramone, S.; Shuey, C.; Cajero, M.; Lewis, J. A Bayesian framework for estimating disease risk due to exposure to uranium mine and mill waste on the Navajo Nation. *J. R. Statist. Soc. Ser. A* **2015**, n/a–n/a.
- (12) Barceloux, D.; Vanadium, G. *Clin. Toxicol.* **1999**, *37* (2), 265–278.
- (13) Campen, M. J.; Nolan, J. P.; Schladweiler, M. C.; Kodavanti, U. P.; Evansky, P. A.; Costa, D. L.; Watkinson, W. P. Cardiovascular and thermoregulatory effects of inhaled PM-associated transition metals: A potential interaction between nickel and vanadium sulfate. *Toxicol. Sci.* **2001**, *64*, 243–252.
- (14) Campen, M. J.; Nolan, J. P.; Schladweiler, M. C. J.; Kodavanti, U. P.; Costa, D. L.; Watkinson, W. P. Cardiac and thermoregulatory effects of instilled particulate matter-associated transition metals in healthy and cardiopulmonary-compromised rats. *J. Toxicol. Environ. Health, Part A* **2002**, *65* (20), 1615–1631.
- (15) Zwolak, I. Vanadium carcinogenic, immunotoxic and neurotoxic effects: a review of in vitro studies. *Toxicol. Mech. Methods* **2014**, *24*, 1–12.
- (16) Mukherjee, B.; Patra, B.; Mahapatra, S.; Banerjee, P.; Tiwari, A.; Chatterjee, M. Vanadium—an element of atypical biological significance. *Toxicol. Lett.* **2004**, *150* (2), 135–143.
- (17) United States Congress.. Uranium Mill Tailings Radiation Control Act of 1978. *Public Law* **1978**, 95–604.
- (18) Stumm, W.; Morgan, J. J. *Aquatic Chemistry, Chemical Equilibria and Rates in Natural Waters*. 3rd ed.; John Wiley & Sons, Inc.: New York, 1996; p 1022.
- (19) Langmuir, D. *Aqueous environmental geochemistry*. 1 ed.; Prentice Hall: Upper Saddle River, NJ, 1997; p 600.
- (20) Maurice, P. A. *Environmental Surfaces and Interfaces from the Nanoscale to the Global Scale*. 1st ed.; John Wiley & Sons, Inc.: Hoboken, NJ, 2009; p 441.
- (21) Fletcher, K. E.; Boyanov, M. I.; Thomas, S. H.; Wu, Q. Z.; Kemner, K. M.; Loffler, F. E. U(VI) reduction to mononuclear U(IV) by desulfobacterium species. *Environ. Sci. Technol.* **2010**, *44* (12), 4705–4709.
- (22) Bernier-Latmani, R.; Veeramani, H.; Vecchia, E. D.; Lezama-Pacheco, J. S.; Suvorova, E. I.; Sharp, J. O.; Wigginton, N. S.; Bargar, J. R. Non-uraninite products of microbial U(VI) reduction. *Environ. Sci. Technol.* **2010**, *44* (24), 9456–9462.
- (23) Cerrato, J. M.; Ashner, M. N.; Alessi, D. S.; Lezama-Pacheco, J. S.; Bernier-Latmani, R.; Bargar, J. R.; Giammar, D. E. Relative reactivity of biogenic and chemogenic uraninite and biogenic noncrystalline U(IV). *Environ. Sci. Technol.* **2013**, *47* (17), 9756–9763.
- (24) Bargar, J. R.; Williams, K. H.; Campbell, K. M.; Long, P. E.; Stubbs, J. E.; Suvorova, E. I.; Lezama-Pacheco, J. S.; Alessi, D. S.; Stylo, M.; Webb, S. M.; Davis, J. A.; Giammar, D. E.; Blue, L. Y.; Bernier-Latmani, R. Uranium redox transition pathways in acetate-amended sediments. *Proc. Natl. Acad. Sci. U. S. A.* **2013**, *110* (12), 4506–4511.
- (25) Anderson, R. T.; Vrionis, H. A.; Ortiz-Bernad, I.; Resch, C. T.; Long, P. E.; Dayvault, R.; Karp, K.; Marutzky, S.; Metzler, D. R.; Peacock, A.; White, D. C.; Lowe, M.; Lovley, D. R. Stimulating the in situ activity of Geobacter species to remove uranium from the groundwater of a uranium-contaminated aquifer. *Appl. Environ. Microbiol.* **2003**, *69* (10), 5884–5891.
- (26) Bargar, J. R.; Bernier-Latmani, R.; Giammar, D. E.; Tebo, B. M. Biogenic uraninite nanoparticles and their importance for uranium remediation. *Elements* **2008**, *4* (6), 407–412.
- (27) Alessi, D. S.; Lezama-Pacheco, J. S.; Janot, N.; Suvorova, E. I.; Cerrato, J. M.; Giammar, D. E.; Davis, J. A.; Fox, P. M.; Williams, K. H.; Long, P. E.; Handley, K. M.; Bernier-Latmani, R.; Bargar, J. R. Speciation and reactivity of uranium products formed during in-situ bioremediation in a shallow alluvial aquifer. *Environ. Sci. Technol.* **2014**, *48* (21), 12842–12850.
- (28) Qafoku, N. P.; Zachara, J. M.; Liu, C. X.; Gassman, P. L.; Qafoku, O. S.; Smith, S. C. Kinetic desorption and sorption of U(VI) during reactive transport in a contaminated Hanford sediment. *Environ. Sci. Technol.* **2005**, *39* (9), 3157–3165.
- (29) Williams, K. H.; Long, P. E.; Davis, J. A.; Wilkins, M. J.; N'Guegan, A. L.; Steefel, C. I.; Yang, L.; Newcomer, D.; Spane, F. A.; Kerkhof, L. J.; McGuinness, L.; Dayvault, R.; Lovley, D. R. Acetate availability and its influence on sustainable bioremediation of uranium-contaminated groundwater. *Geomicrobiol. J.* **2011**, *28* (5–6), 519–539.
- (30) Dong, W. M.; Brooks, S. C. Determination of the formation constants of ternary complexes of uranyl and carbonate with alkaline earth metals ( $Mg^{2+}$ ,  $Ca^{2+}$ ,  $Sr^{2+}$ , and  $Ba^{2+}$ ) using anion exchange method. *Environ. Sci. Technol.* **2006**, *40* (15), 4689–4695.
- (31) Stewart, B. D.; Neiss, J.; Fendorf, S. Quantifying constraints imposed by calcium and iron on bacterial reduction of uranium(VI). *J. Environ. Qual.* **2007**, *36* (2), 363–372.
- (32) Giammar, D. Geochemistry of Uranium at Mineral-Water Interfaces: Rates of Sorption-Desorption and Dissolution-Precipitation Reactions. Ph.D. Dissertation, California Institute of Technology: Pasadena, CA, 2001.
- (33) Wang, Z.; Lee, S.-W.; Catalano, J. G.; Lezama-Pacheco, J. S.; Bargar, J. R.; Tebo, B. M.; Giammar, D. E. Adsorption of Uranium(VI) to Manganese Oxides: X-ray Absorption Spectroscopy and Surface Complexation Modeling. *Environ. Sci. Technol.* **2012**, *47* (2), 850–858.
- (34) Nico, P. S.; Stewart, B. D.; Fendorf, S. Incorporation of Oxidized Uranium into Fe (Hydr)oxides during Fe(II) Catalyzed Remineralization. *Environ. Sci. Technol.* **2009**, *43* (19), 7391–7396.
- (35) Massey, M. S.; Lezama-Pacheco, J. S.; Jones, M. E.; Ilton, E. S.; Cerrato, J. M.; Bargar, J. R.; Fendorf, S. Competing retention pathways

- of uranium upon reaction with Fe(II). *Geochim. Cosmochim. Acta* **2014**, *142*, 166–185.
- (36) Gorman-Lewis, D.; Burns, P. C.; Fein, J. B. Review of uranyl mineral solubility measurements. *J. Chem. Thermodyn.* **2008**, *40* (3), 335–352.
- (37) Burns, P. C. U6+ minerals and inorganic compounds: insights into an expanded structural hierarchy of crystal structures. *Can. Mineral.* **2005**, *43* (6), 1839–1894.
- (38) Tokunaga, T. K.; Kim, Y.; Wan, J. Potential remediation approach for uranium-contaminated groundwaters through potassium uranyl vanadate precipitation. *Environ. Sci. Technol.* **2009**, *43* (14), S467–S471.
- (39) Tokunaga, T. K.; Kim, Y.; Wan, J.; Yang, L. Aqueous Uranium(VI) Concentrations Controlled by Calcium Uranyl Vanadate Precipitates. *Environ. Sci. Technol.* **2012**, *46* (14), 7471–7477.
- (40) Alam, M. S.; Cheng, T. Uranium release from sediment to groundwater: Influence of water chemistry and insights into release mechanisms. *J. Contam. Hydrol.* **2014**, *164*, 72–87.
- (41) Neil, C. W.; Yang, Y. J.; Schupp, D.; Jun, Y.-S. Water Chemistry Impacts on Arsenic Mobilization from Arsenopyrite Dissolution and Secondary Mineral Precipitation: Implications for Managed Aquifer Recharge. *Environ. Sci. Technol.* **2014**, *48* (8), 4395–4405.
- (42) Kim, C. S.; Chi, C.; Miller, S. R.; Rosales, R. A.; Sugihara, E. S.; Akau, J.; Rytuba, J. J.; Webb, S. M. (Micro)spectroscopic Analyses of Particle Size Dependence on Arsenic Distribution and Speciation in Mine Wastes. *Environ. Sci. Technol.* **2013**, *47* (15), 8164–8171.
- (43) Nesbitt, H.; Muir, I. Oxidation states and speciation of secondary products on pyrite and arsenopyrite reacted with mine waste waters and air. *Mineral. Petrol.* **1998**, *62* (1–2), 123–144.
- (44) Foster, A. L.; Brown, G. E., Jr.; Tingle, T. N.; Parks, G. A. Quantitative arsenic speciation in mine tailings using X-ray absorption spectroscopy. *Am. Mineral.* **1998**, *83* (5), 553–568.
- (45) Dixit, S.; Hering, J. G. Comparison of Arsenic(V) and Arsenic(III) Sorption onto Iron Oxide Minerals: Implications for Arsenic Mobility. *Environ. Sci. Technol.* **2003**, *37* (18), 4182–4189.
- (46) Moldovan, B. J.; Jiang, D. T.; Hendry, M. J. Mineralogical Characterization of Arsenic in Uranium Mine Tailings Precipitated from Iron-Rich Hydrometallurgical Solutions. *Environ. Sci. Technol.* **2003**, *37* (5), 873–879.
- (47) Fendorf, S.; Michael, H. A.; van Geen, A. Spatial and temporal variations of groundwater arsenic in South and Southeast Asia. *Science* **2010**, *328* (5982), 1123–1127.
- (48) Borch, T.; Kretzschmar, R.; Kappler, A.; Van Cappellen, P.; Ginder-Vogel, M.; Voegelin, A.; Campbell, K. Biogeochemical Redox Processes and their Impact on Contaminant Dynamics. *Environ. Sci. Technol.* **2010**, *44* (1), 15–23.
- (49) Ying, S. C.; Kocar, B. D.; Fendorf, S. Oxidation and competitive retention of arsenic between iron- and manganese oxides. *Geochim. Cosmochim. Acta* **2012**, *96* (0), 294–303.
- (50) Troyer, L. D.; Tang, Y.; Borch, T. Simultaneous Reduction of Arsenic(V) and Uranium(VI) by Mackinawite: Role of Uranyl Arsenate Precipitate Formation. *Environ. Sci. Technol.* **2014**, *48* (24), 14326–14334.
- (51) Mandaliev, P. N.; Mikutta, C.; Barmettler, K.; Kotsev, T.; Kretzschmar, R. Arsenic Species Formed from Arsenopyrite Weathering along a Contamination Gradient in Circumneutral River Floodplain Soils. *Environ. Sci. Technol.* **2013**, *48* (1), 208–217.
- (52) Smedley, P. L.; Kinniburgh, D. G. A review of the source, behaviour and distribution of arsenic in natural waters. *Appl. Geochem.* **2002**, *17* (5), 517–568.
- (53) Donahue, R.; Hendry, M. Geochemistry of arsenic in uranium mine mill tailings, Saskatchewan, Canada. *Appl. Geochem.* **2003**, *18* (11), 1733–1750.
- (54) U.S. EPA, *National Primary Drinking Water Regulations; Arsenic and Clarifications to Compliance and New Source Contaminants Monitoring*; Final Rule. In Federal Register, Vol. 66, No. 14, 2001; p 6976.
- (55) Zachara, J. M.; Long, P. E.; Bargar, J.; Davis, J. A.; Fox, P.; Fredrickson, J. K.; Freshley, M. D.; Konopka, A. E.; Liu, C.; McKinley, J. P.; Rockhold, M. L.; Williams, K. H.; Yabusaki, S. B. Persistence of uranium groundwater plumes: Contrasting mechanisms at two DOE sites in the groundwater–river interaction zone. *J. Contam. Hydrol.* **2013**, *147* (0), 45–72.
- (56) Franczyk, K. J. *Stratigraphic revision and depositional environments of the Upper Cretaceous Toreva Formation in the northern Black Mesa area, Navajo and Apache Counties, Arizona*. U.S. Geological Survey: Reston, VA, 1988.
- (57) Chenoweth, W. L. *The geology and production history of the uranium deposits in the Toreva Formation*; Arizona Geological Survey: Black Mesa, Apache County, Arizona, 1990; Contributed Report 90-A.
- (58) Dreesen, D. R.; Williams, J. M.; Marple, M. L.; Gladney, E. S.; Perrin, D. R. Mobility and bioavailability of uranium mill tailings contaminants. *Environ. Sci. Technol.* **1982**, *16* (10), 702–709.
- (59) Campbell, K. M.; Kukkadapu, R. K.; Qafoku, N.; Peacock, A. D.; Lesher, E.; Williams, K. H.; Bargar, J. R.; Wilkins, M. J.; Figueroa, L.; Ranville, J. Geochemical, mineralogical and microbiological characteristics of sediment from a naturally reduced zone in a uranium-contaminated aquifer. *Appl. Geochem.* **2012**, *27* (8), 1499–1511.
- (60) U.S. Code of Federal Regulations, 10CFR40.4(h). In Federal Government, U.S. Government Publishing Office: Washington, D.C., 2014.